Title

FOXL2C134W-Induced CYP19 Expression via Cooperation With SMAD3 in HGrC1 Cells.

Journal

Endocrinology, 159(4)

ISSN

0888-8809

Authors

Belli, Martina
Iwata, Nahoko
Nakamura, Tomoko
et al.

Publication Date

2018-04-01

DOI

10.1210/en.2017-03207

FOXL2^{C134W}-Induced CYP19 Expression via Cooperation With SMAD3 in HGrC1 Cells

Martina Belli,[1] Nahoko Iwata,[1] Tomoko Nakamura,[2] Akira Iwase,[2] Dwayne Stupack,[1] and Shunichi Shimasaki[1]

[1]Department of Reproductive Medicine, School of Medicine, University of California, San Diego, La Jolla, California 92093; and [2]Center for Maternal-Perinatal Care, Nagoya University Hospital, Nagoya 466-8560, Japan

Germline knockout studies in female mice demonstrated an essential role for forkhead box L2 (FOXL2) in early follicle development, whereas an inducible granulosa cell (GC)–specific deletion of *Foxl2* in adults has shown ovary-to-testis somatic sex reprogramming. In women, over 120 different germline mutations in the *FOXL2* gene have been shown to cause blepharophimosis/ptosis/epicantus inversus syndrome associated with or without primary ovarian insufficiency. By contrast, a single somatic mutation (*FOXL2^{C134W}*) accounts for almost all adult-type GC tumors (aGCTs). To test the hypothesis that FOXL2^{C134W} differentially regulates the expression of aGCT markers, we investigated the effect of FOXL2^{C134W} on inhibin B and P450 aromatase expression using a recently established human GC line (HGrC1), which we now show to bear two normal alleles of *FOXL2*. Neither FOXL2^{wt} nor FOXL2^{C134W} regulate INHBB messenger RNA (mRNA) expression. However, FOXL2^{C134W} selectively displays a 50-fold induction of CYP19 mRNA expression dependent upon activin A. Mechanistically, the *CYP19* promoter is activated in a similar way by FOXL2^{C134W} interaction with SMAD3, but not by FOXL2^{wt}. SMAD2 had no effect. Moreover, FOXL2^{C134W} interactions with SMAD3 and with the FOX binding element located at –199 bp upstream of the ATG initiation codon of *CYP19* are more sustainable than FOXL2^{wt}. Thus, FOXL2^{C134W} potentiates CYP19 expression in HGrC1 cells via enhanced recruitment of SMAD3 to a proximal FOX binding element. These findings may explain the pathophysiology of estrogen excess in patients with aGCT. (***Endocrinology*** **159: 1690–1703, 2018)**

The forkhead box L2 (FOXL2) is an evolutionarily conserved member of the forkhead transcription factor family (1). Histological studies in humans, mice, and goats have detected FOXL2 messenger RNA (mRNA) and protein in the mesenchyme of developing eyelids, fetal and adult granulosa cells (GCs) of the ovary, embryonic as well as adult pituitary gonadotrope and thyrotroph cells of the pituitary, and endometrium of the uterus (1–8). Two *Foxl2* germline null mouse models generated in different laboratories demonstrated high perinatal mortality (50% to 95%), most likely associated with coincident craniofacial defects (7, 9). However, the surviving mice confirmed a critical role of FOXL2 in ovarian function, with a block in follicle development at the primary stage associated with a failure of GCs to complete the squamous-to-cuboidal transition. In contrast, the inducible somatic deletion of *Foxl2* in GCs of adult mouse ovarian follicles led to the ovary-to-testis somatic sex reprogramming associated with the transdifferentiation of mature granulosa/theca cells into Sertoli/Leydig-like cells as well as the upregulation of genes involved in testis determination vs the downregulation of ovary-specific genes, such as P450 aromatase (CYP19) (10). Thus, FOXL2 appeared to be essential for the maintenance of the female gonadal sex throughout mouse life.

In humans, mutations in the *FOXL2* gene are involved in diverse ovarian dysfunctions. More than 120 germline mutations of *FOXL2* have been related to

ISSN Online 1945-7170

Received 4 December 2017. Accepted 13 February 2018.
First Published Online 19 February 2018

Abbreviations: aGCT, adult-type granulosa cell tumor; BPES, blepharophimosis/ptosis/epicantus inversus syndrome; CHO, Chinese hamster ovary; Co-IP, coimmunoprecipitation; DMEM, Dulbecco's modified Eagle medium; E_2, estradiol; FBE, FOX binding element; FOXL2, forkhead box L2; GC, granulosa cell; GCT, granulosa cell tumor; mRNA, messenger RNA; PCR, polymerase chain reaction; qRT-PCR, quantitative reverse transcription polymerase chain reaction; RRID, Research Resource Identifier; SBE, SMAD binding element; SEM, standard error of the mean; SF1, steroid factor 1.

blepharophimosis/ptosis/epicantus inversus syndrome (BPES) associated with or without primary ovarian insufficiency (BPES type I and type II, respectively) (2, 11). BPES type I typically results from FOXL2 truncations predicted to result in loss of function, whereas type II BPES mutations are generally hypomorphic and do not result in ovarian dysfunction (12, 13). In striking contrast, a single somatic mutation, *FOXL2*^{C134W}, which was not found in BPES, was detected in almost all adult-type GC tumors (aGCTs) (14), as collected from more than 400 patients of various ethnicities (15). Although accumulating evidence suggested that FOXL2^{C134W} is a strong driver candidate in the pathogenesis of aGCTs (11, 16–21), the molecular basis of FOXL2^{C134W} action in regulating GC tumorigenesis is largely unknown.

FOXL2 regulates the transcription of various genes involved in diverse cellular processes such as steroidogenesis (*e.g.*, *STAR* and *CYP19*), steroid metabolism (*PPARGC1A* and *NR5A2*), metabolism of reactive oxygen species (*MnSOD* or *SOD2*), stress response (*SIRT1*), cell cycle (*CCND2*, *CCNA2*, and *P16/INK4a*), and DNA repair (*GADD45A* and *ALKBH8*) (6, 22–27). In particular, FOXL2 regulation of CYP19 has been known across a variety of vertebrate species, including human, rodent, goat, fish, chicken, and frog (27). The specificity of action of FOXL2 on such a wide spectrum of cellular functions is likely governed by its interaction with cofactors. Steroid factor 1 (SF1) is a key factor in steroidogenesis, as it regulates *CYP11*, *CYP17*, *CYP19*, and *STAR* (28). FOXL2 prevents SF1 binding to the *CYP17* promoter, leading to the suppression of SF1-induced CYP17 expression (29). In contrast, FOXL2 associates with SF1 and together enhance *CYP19* promoter activity.

Interestingly, it was postulated that this dual regulation could play a role in the balance of androgen and estrogen biosynthesis (27, 29). The DEAD-box protein DP103 is a regulator of SF1 (30), which interacts with FOXL2 to induce apoptosis in Chinese hamster ovary (CHO) cells and rat primary GCs (31, 32). Whether an abnormal FOXL2-DP103 interaction may explain FOXL2^{C134W}-mediated reduction in apoptotic potential is unknown (33, 34). FOXL2 also interacts with estrogen receptor α (35) and inhibits the activation of the *PTGS2* promoter by estrogen receptor α (10, 35). Another partner of FOXL2 is SMAD3, which interacts with it to regulate *GnRHR* promoter in the pituitary (36). Also within the pituitary, FOXL2 interacts with SMAD3 to stimulate *FSHB* and *FST* promoter activities (37–39), and a similar interaction in regulating *FST* transcription was later confirmed in GCs (40, 41). An emerging and important molecular basis underlying the pathogenesis of GC tumors (GCTs) is an alteration in the SMAD3/FOXL2 interaction (42).

Many studies that investigate the role of FOXL2^{C134W} in GCs use immortalized human GC lines, either KGN (16, 24, 43–55) or COV434 cells (16, 40, 46, 48, 49, 52, 53, 56). The KGN cell line is derived from a postmenopausal woman with an aGCT (57), whereas the COV434 cell line is from a 27-year-old woman (58) considered to have a juvenile GCT. In the current study, we used the HGrC1 cell line recently established by lentiviral-mediated transfer of immortalizing genes into human primary GCs derived from a normal right ovary of a 35-year-old woman (59). HGrC1 cells are nonluteinized GCs that maintain expression of functional receptors for gonadotropins and TGF-β superfamily members (activin, BMP4, BMP6, BMP7, GDF9, and AMH) as well as steroidogenic factors (StAR, CYP11, and CYP19).

A long-term goal of our study is to determine whether and how the *FOXL2*^{C134W} mutation is involved in the etiology and/or progression of aGCTs. Toward this goal, we have evaluated potential cooperation among SMAD3 and FOXL2 in regulating expression of aGCT markers (21), following the hypothesis that FOXL2^{C134W} functions differently than FOXL2^{wt}. Specifically, we have focused on inhibin B and CYP19 as FOXL2 targets and investigated whether and how FOXL2^{wt} and FOXL2^{C134W} differentially regulate expression of these genes in association with SMAD3.

Materials and Methods

Plasmids and reagents

Activin A was produced in our laboratory as previously described (60). Antibodies against SMAD2/SMAD3 [catalog no. 3102; Research Resource Identifier (RRID): AB_10698742] and β-actin (catalog no. 4967; RRID: AB_330288) were purchased from Cell Signaling Technology (Danvers, MA). The antibody against FOXL2 (catalog no. IMG-3228; RRID: AB_613022) was purchased from Imgenex (San Diego, CA), the antibody against FLAG tag (catalog no. F1804; RRID: AB_262044) from Sigma-Aldrich (St. Louis, MO), and the antibody against c-Myc tag (catalog no. 551101; RRID: AB_394046) from BD Pharmingen (Franklin Lakes, NJ). Establishment of the HGrC1 cell line was reported (59). An expression plasmid encoding N-terminally Flag-tagged human FOXL2^{wt} (FOXL2^{wt}) was kindly provided by Dr. Louise Bilezikjian (37), and its mutant (FOXL2^{C134W}) was constructed in our laboratory as previously described (40, 41). Expression plasmids encoding human SMAD2 and SMAD3 with or without N-terminal Myc tags were prepared from those kindly provided by Drs. Kohei Miyazono (61, 62) and Louise Bilezikjian (37). Luciferase reporter plasmids with different lengths of human CYP19 promoter were constructed in our laboratory using polymerase chain reaction (PCR)–based methods. Biotinylated oligonucleotide probes were purchased from Integrated DNA Technologies (San Diego, CA).

HGrC1 cells culture

HGrC1 cells were cultured at 37°C in Dulbecco's modified Eagle medium (DMEM)–F12 medium (catalog no. 12400-024; Thermo Fisher Scientific, Waltham, MA) supplemented with 10% fetal bovine serum (catalog no. F6178; Sigma-Aldrich) and antibiotics (penicillin and streptomycin). All the experiments in this study were performed using HGrC1 cells at passage 14. For some experiments, HGrC1 cells were treated with 100 ng/mL activin A for 24 hours in serum-free DMEM-F12 medium.

FOXL2 gene sequencing

Genomic DNA from 5×10^6 HGrC1 cells was extracted using the GenElute Mammalian Genomic DNA Miniprep Kit (catalog no. G1N70; Sigma-Aldrich). Because human *FOXL2* gene is extremely rich in GC (>84% in part), we amplified several short DNA segments overlapping in the entire coding sequence of the gene by PCR using two different DNA polymerases, Phusion Hot Start Flex DNA Polymerase (catalog no. M0535S; New England BioLabs, Ipswich, MA) and Platinum SuperFi DNA Polymerase (catalog no. 12351010; Thermo Fisher Scientific), following the manufacturer's protocols. The following PCR primers were used: (1) forward primer 5′-CGTGCGCCCCAACTCTTTGCC-3′ and reverse primer 5′-GGATCGCCATGGCGATGAGCG-3′; (2) forward primer 5′-GCGCCGGCTTTGTCATGATG-3′ and reverse primer 5′-GCCGGAAGGGCCTCTTCATG-3′; (3) forward primer 5′-GAAGACATGTTCGAGAAGGG-3′ and reverse primer 5′-GTGTGTACGGCCCGTACGAG-3′; (4) forward primer 5′-GGCTTCCTCAACAACTCGTG-3′ and reverse primer 5′-TTGTACGAGTTCACTACGCC-3′; (5) forward primer 5′-CTATGCCTCCTGCCAGATGG-3′ and reverse primer 5′-TTGTACGAGTTCACTACGCC-3′; (6) forward primer 5′-GCCTGCAGTTCGCTTGTGCC-3′ and reverse primer 5′-CGTCCCTGCATCCTCGCATC-3′; (7) forward primer 5′-GATGCATTGCTCTTACTGGG-3′ and reverse primer 5′-TGCAAGGTCACAGAGGTCAG-3′; (8) forward primer 5′-ATCCGCACGCACACCATCTG-3′ and reverse primer 5′-CCCAGTAAGAGCAATGCATC-3′; and (9) forward primer 5′-TACACACGCGTGCAGAGCATG-3' and reverse primer 5′-CTGGGCTGGCAGGGCTGAGCTG-3′. PCR products were extracted from gel, purified, and sequenced (Genewiz, San Diego, CA).

Transient transfections

HGrC1 cells were plated into either 12-well tissue culture plates at a density of 0.5×10^6 cells per well or 6-well tissue culture plates at a density of 1×10^6 cells/well. The next day, the medium was replaced with serum-free DMEM-F12 (supplemented with antibiotics), and transfection was performed with the previously described plasmids for 4 hours using Lipofectamine LTX with Plus Reagent (catalog no. 15338100; Thermo Fisher Scientific) following manufacturer's procedures. After 4 hours, medium was replaced with new serum-free DMEM-F12 and transfected cells were cultured at 37°C for 24 hours with or without activin A. Cells were then lysed for further analyses.

RNA extractions and quantitative reverse transcription PCR

After 4-hour transfection and an additional 24-hour culture, HGrC1 cells were lysed in TRIzol reagent (catalog no. 15596026; Thermo Fisher Scientific), and RNA was extracted using the Direct-zol RNA MiniPrep Kit (catalog no. R2052; Zymo Research, Irvine, CA) following manufacturer's protocol. RNA (1 μg) was reverse transcribed using the High-Capacity cDNA Reverse Transcription Kit (catalog no. 4368814; Thermo Fisher Scientific), and complementary DNA was used to quantify mRNA expression by quantitative reverse transcription PCR (qRT-PCR) using SYBR Green PCR Master Mix (catalog no. 4309155; Thermo Fisher Scientific) and the 7300 Real-Time PCR System Thermal Cycler (Applied Biosystems, Foster City, CA). The following primer sequences were used: CYP19, forward primer 5′-GGAATTATGAGGGCACATCC-3′ and reverse primer 5′-GTTGTAGTAGTTGCAGGCAC-3′; INHBB, forward primer 5′-CGCGTTTCCGAAATCATCAG-3′ and reverse primer 5′-GTTTCAGGTAAAGCCACAGG-3′; and L19, forward primer 5′-GGGATTTGCATTCAGAGATCAG-3′ and reverse primer 5′-GGAAGGGCATCTCGTAAG-3′. Target gene expressions were normalized on L19 expression.

Western blot analysis

After 4-hour transfection and 24-hour culture at 37°C, HGrC1 cells were lysed in lysis buffer (radioimmunoprecipitation assay buffer; catalog no. 89901; Thermo Fisher Scientific), phosphatase inhibitor cocktail (catalog no. 78420; Thermo Fisher Scientific), and protease inhibitor cocktail (catalog no. P8340; Sigma-Aldrich), and total protein content was quantified with the Pierce BCA Protein Assay Kit (catalog no. 23227; Thermo Fisher Scientific). NuPAGE LDS Sample Buffer (4X) (catalog no. NP0007; Thermo Fisher Scientific) and β-mercaptoethanol (catalog no. 6010; Calbiochem, Billerica, MA) were added to cell lysates, and samples were heated to 95°C for 5 minutes for protein denaturation. Cell lysates were separated on 12% sodium dodecyl sulfate–polyacrylamide gel electrophoresis gels and then transferred to nitrocellulose membranes. The membranes were incubated for 1 hour with blocking solution (bovine serum albumin; catalog no. A30075-100; Research Products International, Mount Prospect, IL) and then with primary antibodies overnight at 4°C. Membranes were washed three times, incubated with horseradish peroxidase–conjugated secondary antibodies for 1 hour, washed three further times, and incubated with Super Signal West Femto Maximum Sensitivity Substrate for chemiluminescence detection (catalog no. 34095; Thermo Fisher Scientific). Alternatively, incubation of membranes in primary and secondary antibodies was performed in Signal Enhancer HIKARI solutions 1 and 2, respectively (nos. NU00101 and NU00102; Nacalai USA, San Diego, CA) to enhance protein detection. β-actin was used as a loading control.

Immunoassay

The E_2 Immunoassay Kit (catalog no. 582251; Caymen Chemical, Ann Arbor, MI) was used to measure estradiol (E_2) levels in culture media from HGrC1 cells transfected with either FOXL2^{wt} or FOXL2^{C134W} in the presence of androstenedione (100 nM), with or without activin A (100 ng/mL). After 4-hour transfection and 48-hour culture at 37°C, culture media from different treatments were collected in glass tubes and spun down to remove cell debris. E_2 was measured using a Bio Tek microplate reader (Bio Tek, Winooski, VT) following manufacturer's instructions.

Luciferase reporter assay

After 4-hour transfection and 24-hour culture at 37°C, HGrC1 cells (0.5×10^6 cells/sample) were lysed in lysis solution

(100 mM potassium phosphate, pH 7.8, 0.2% Triton X-100), and luciferase reporter assay was performed using Dual-Light Luciferase & β-Galactosidase Reporter Gene Assay System (catalog no. T1003; Thermo Fisher Scientific) following manufacturer's instructions. Relative firefly luciferase activity was measured with the FLUOstar Omega Microplate Reader (BMG Labtech, Ortenberg, Germany) and normalized by β-galactosidase activity.

Coimmunoprecipitation and oligonucleotide precipitation assays

After 4-hour transfection and 24-hour culture at 37°C, HGrC1 cells [2.5×10^6 cells/sample for coimmunoprecipitation (Co-IP) assay; 5×10^6 cells/sample for oligonucleotide precipitation assay] were lysed in lysis solution [25 mM tris (hydroxymethyl)aminomethane-HCl, pH 7.4, 140 mM NaCl, 1 mM EDTA, 0.1% NP-40, 0.5% Triton X-100, 10% glycerol, 2 mM NaF, and freshly added 1 mM $Na_4P_2O_7$ and protease inhibitor cocktail (catalog no. P8340; Sigma-Aldrich)]. Cell extracts were sonicated two times for 3 to 4 seconds each and centrifuged at 4°C for 10 minutes at 13,000 rpm, and supernatants were collected. For Co-IP assay, supernatants were precleared with mouse immunoglobulin G agarose (catalog no. A0919) for 1 hour, and then immunoprecipitations were performed with anti-FLAG M2 affinity gel (catalog no. A2220; Sigma-Aldrich) overnight at 4°C. The precipitants were washed three times in lysis buffer and eluted with FLAG peptide (catalog no. F3290; Sigma-Aldrich). Western blot analysis was performed to detect coprecipitating SMAD3 and FOXL2 proteins with anti-Myc and anti-Flag antibodies, respectively. For the oligonucleotide precipitation assay, 2 μg of biotinylated oligonucleotides were precoupled to streptavidin agarose (catalog no. 20353; Thermo Fisher Scientific) at 4°C for 1 hour and subsequently incubated with cell lysates together with 8 μg of poly(deoxyinosinic-deoxycytidylic) (catalog no. P4929; Sigma-Aldrich) at 4°C for 2 hours. Cell lysates were washed three times in lysis buffer and eluted with NuPage LDS Sample Buffer (catalog no. NP0007; Thermo Fisher Scientific). Immunoblot analysis was performed to detect FOXL2 proteins via the anti-Flag antibody. Resolved band intensity was quantified using Image Laboratory Software from Bio-Rad (Hercules, CA).

Statistic analysis

Data analysis was performed with JMP Pro 12 software (Cary, NC) using Box-Cox transformation and one-way analysis of variance with least-squares means Tukey honest significant difference test or least-squares means Student *t* test. Significance was set at $P < 0.05$, and data are shown as mean ± standard error of the mean (SEM).

Results

The coding sequence of the *FOXL2* gene in HGrC1 cells is normal

Prior to implementation of the HGrC1 cell line in this study, chromosome DNA extracted from HGrC1 cells was subjected to PCR to determine the DNA sequence of the *FOXL2* gene. Although human FOXL2 gene is extremely rich in GC (>84% in some regions), we were able to determine the entire coding regions of the *FOXL2* genes at both alleles, confirming they were intact and lacked mutation (data not shown).

FOXL2^{C134W}, but not FOXL2^{wt}, is a remarkable inducer of CYP19 mRNA expression in HGrC1 cells when treated with activin A

HGrC1 cells were transfected with either FOXL2^{wt} or FOXL2^{C134W} plasmid, or their empty vector as a control. Cell lysates were collected and total protein content was measured to use equal amounts of proteins for sodium dodecyl sulfate–polyacrylamide gel electrophoresis analysis. The inset in Fig. 1(a) shows the relative expression levels of endogenous FOXL2, exogenous FOXL2^{wt} and FOXL2^{C134W} (top panel), and β-actin (bottom panel). Both FOXL2^{wt} and FOXL2^{C134W} proteins were expressed at comparable levels with elevated levels (>12-fold) relative to endogenous FOXL2 (which is almost invisible in this blot, but clearly detectable at longer exposures; data not shown). Cells were transfected and treated with or without activin A (100 ng/mL) for 24 hours to evaluate CYP19 and INHBB mRNA expression. Total RNA was then collected, and expression was analyzed by qRT-PCR [Fig. 1(a) and 1(b)]. Neither activin A nor FOXL2^{wt}, alone or together, influenced CYP19 mRNA expression compared with controls. However, in the absence of activin A, FOXL2^{C134W} demonstrated a very small but significant induction of CYP19 mRNA expression relative to control (approximately twofold; $P < 0.05$). Strikingly, in the presence of activin A, a remarkable induction (50-fold) was observed ($P < 0.05$). In contrast, FOXL2^{wt}, FOXL2^{C134W}, and activin A did not significantly regulate INHBB mRNA expression. To test whether CYP19 mRNA overexpression could lead to an increased aromatase activity, E_2 levels were measured in culture media from HGrC1 cells transfected with either FOXL2^{wt} or FOXL2^{C134W} and treated with androstenedione (100 nM), with or without activin A (100 ng/mL), for 48 hours. In agreement with the CYP19 mRNA data, a significant increase in E_2 (20-fold relative to control) was observed when HGrC1 cells were treated with androstenedione and activin A in the presence of FOXL2^{C134W} ($P < 0.05$), but not FOXL2^{wt} [Fig. 1(c)]. These results support the contention that FOXL2^{C134W} acts as a strong stimulator of CYP19 mRNA expression, and aromatase activity, in HGrC1 cells treated with activin A.

SMAD3 is involved in FOXL2^{C134W} induction of CYP19 mRNA expression, but not of INHBB, in HGrC1 cells

To investigate whether the FOXL2^{C134W} induction of CYP19 cooperated with SMAD3, a downstream transducer of activin A signaling, HGrC1 cells were transfected

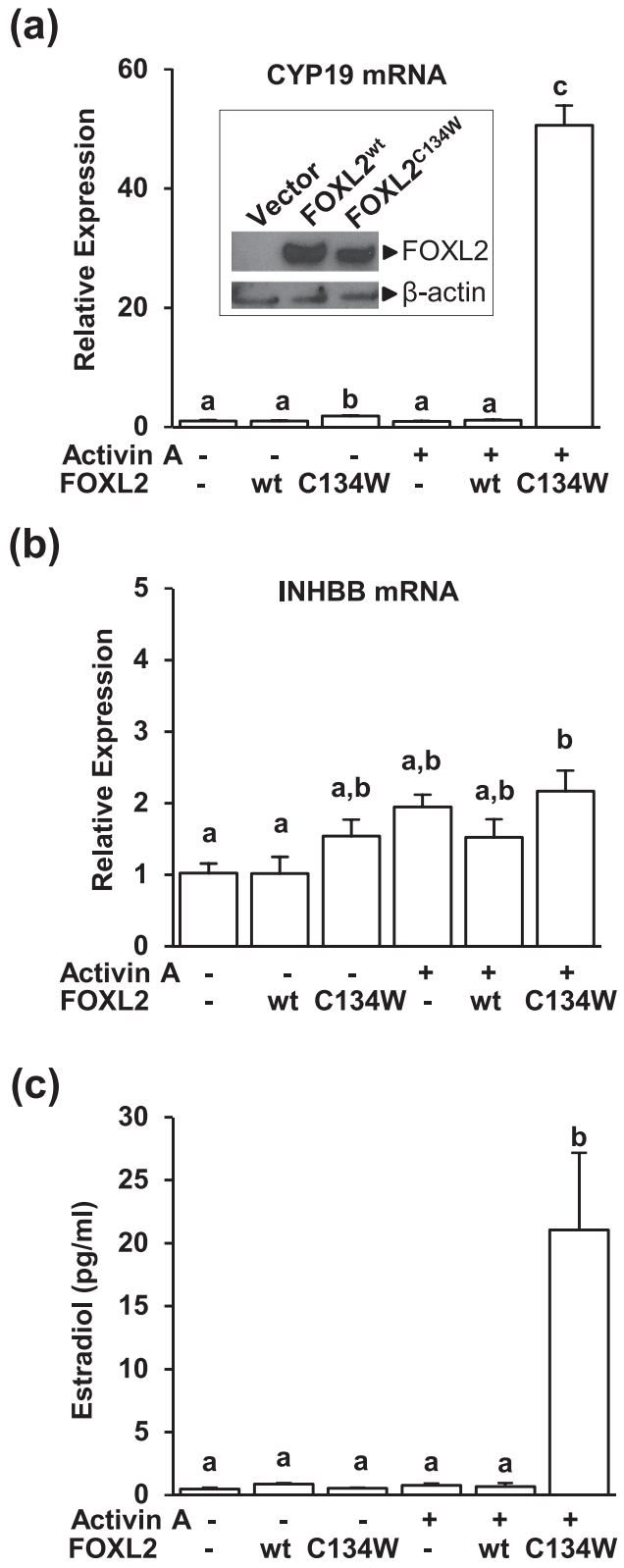

Figure 1. Effects of FOXL2^{wt} and FOXL2^{C134W} on the CYP19 and INHBB mRNA expression and E_2 production in the presence or absence of activin A in HGrC1 cells. HGrC1 cells were transfected with or without 500 ng of Flag-FOXL2^{wt} or Flag-FOXL2^{C134W} plasmids or their empty vector. After 4 hours, serum-free medium was replaced, and cells were cultured in the presence or absence of 100 ng/mL activin A for 24 hours followed by the collection of cell lysates and total RNA. (Inset) Cell lysates were subjected to western blot analysis to show the expression levels of Flag-FOXL2^{wt} or Flag-FOXL2^{C134W} proteins. Antibodies against FOXL2 and β-actin (for loading control) were used. Representative results from duplicate experiments are shown. Total RNA was used to measure (a) CYP19 or (b) INHBB mRNA levels by qRT-PCR. For E_2 level measurement, transfected cells were cultured in the presence of 100 nM androstenedione, with or without 100 ng/mL activin A for 48 hours followed by the collection of culture media. (c) E_2 levels are shown (pg/mL). Representative results (n = 3) from triplicate experiments are presented. Data are shown as mean ± SEM. Different letters denote significant difference among experimental conditions ($P < 0.05$). wt, wild-type.

singly or using combinations of SMAD3, FOXL2^{wt}, and FOXL2^{C134W} plasmids and their empty vectors. The inset in Fig. 2(a) shows the endogenous and ectopically expressed (on average, 2.3-fold) levels of SMAD3 protein. We noted that the overexpressed SMAD3 levels are comparable to endogenous SMAD2 levels, emphasizing the high level of endogenous expression of SMAD2 in HGrC1 cells [insets in Fig. 2(a) and Fig. 3]. FOXL2^{wt} did not influence CYP19 mRNA expression [Fig. 2(a)]. As previously observed, FOXL2^{C134W} (without SMAD3) slightly but significantly induced CYP19 mRNA expression. However, when SMAD3 was ectopically expressed, FOXL2^{C134W} coexpressing cells increased CYP19 mRNA expression by eightfold compared with the control ($P < 0.05$), whereas coexpression with FOXL2^{wt} had no effect on CYP19 levels. In Fig. 2(b), INHBB mRNA levels were measured, but neither FOXL2^{wt}, FOXL2^{C134W}, nor SMAD3 regulated INHBB mRNA. These results indicate that SMAD3 mediates the stimulatory effect of FOXL2^{C134W} on CYP19 expression in HGrC1 cells.

SMAD2 does not enhance FOXL2^{C134W}-mediated induction of CYP19 mRNA expression in HGrC1 cells

Because SMAD2 is also a signal transducer of activin A, we tested whether SMAD2 expression influences FOXL2^{C134W}-mediated induction of CYP19 mRNA expression. HGrC1 cells were transfected singly or using combinations of SMAD2, FOXL2^{wt}, and FOXL2^{C134W} plasmids and their empty vectors. The inset in Fig. 3 shows the endogenous and overexpressed (on average, 1.7-fold) levels of SMAD2 protein. Endogenous SMAD2 is higher than SMAD3 in HGrC1 cells [insets in Fig. 2(a) and Fig. 3]. Nonetheless, no difference in CYP19 mRNA levels between FOXL2^{wt} or FOXL2^{C134W} treatments (Fig. 3, lanes 2 and 3) was observed. Further, elevating the expression of SMAD2 did not alter these results (Fig. 3, lanes 5 and 6). These data identify SMAD3 as selectively exerting a synergistic effect with FOXL2^{C134W} on the stimulation of CYP19 mRNA expression in HGrC1 cells.

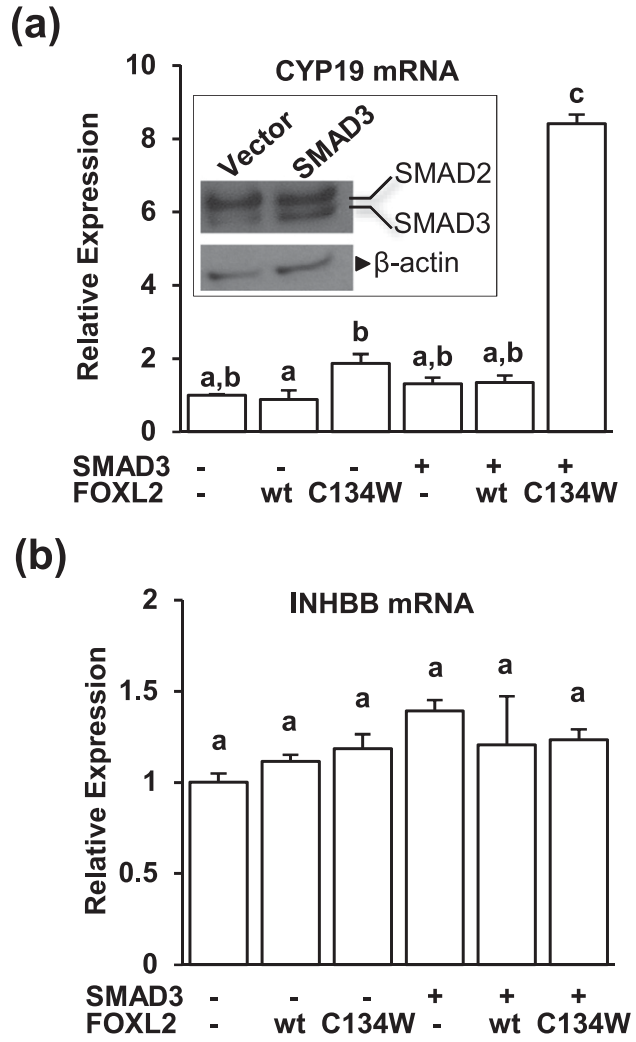

Figure 2. Effects of FOXL2^{wt} and FOXL2^{C134W} on the CYP19 and INHBB mRNA expression with or without SMAD3 overexpression in HGrC1 cells. HGrC1 cells were transfected with or without 500 ng of SMAD3, Flag-FOXL2^{wt}, and Flag-FOXL2^{C134W} plasmids, alone or in combination. Empty expression vectors for SMAD3 and for Flag-FOXL2 were added as necessary to equalize the amount of plasmid transfected per well. After 4 hours, serum-free medium was replaced and cells were cultured for 24 hours. (Inset) Western blot analysis was performed to show the expression levels of SMAD3 protein. Antibodies against SMAD2/SMAD3 and β-actin (for loading control) were used. Representative results from duplicate experiments are shown. qRT-PCR was performed to measure (a) CYP19 and (b) INHBB mRNA levels. Representative results (n = 3) from triplicate experiments are presented. Data are shown as mean ± SEM. Different letters denote significant difference among experimental conditions ($P < 0.05$). wt, wild-type.

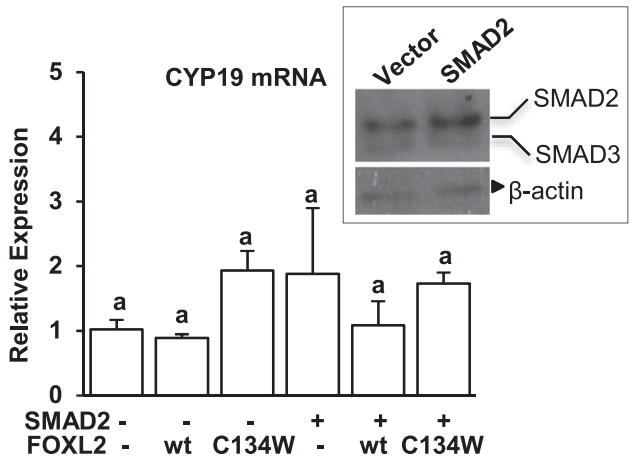

Figure 3. Effects of FOXL2^{wt} and FOXL2^{C134W} on the CYP19 mRNA expression with or without SMAD2 overexpression. HGrC1 cells were transfected with or without 500 ng of Myc-SMAD2, Flag-FOXL2^{wt}, and Flag-FOXL2^{C134W} plasmids, alone or in combination. Empty expression vectors for Myc-SMAD2 and for Flag-FOXL2 were added as necessary to equalize the amount of plasmid transfected per well. After 4 hours, serum-free medium was replaced and cells were cultured for 24 hours. (Inset) Western blot analysis was performed to show the expression levels of SMAD2 protein. Antibodies against SMAD2/SMAD3 and β-actin (for loading control) were used. Representative results from duplicate experiments are shown. qRT-PCR was performed to measure CYP19 mRNA levels. Representative results (n = 3) from triplicate experiments are presented. Data are shown as mean ± SEM. Equal letters denote a nonsignificant difference among experimental conditions ($P < 0.05$). wt, wild-type.

FOXL2^{C134W}, together with SMAD3, significantly induces CYP19 promoter activity

Prior to testing the ability of FOXL2^{wt} or FOXL2^{C134W} to regulate *CYP19* transcription, the human *CYP19* promoter region was analyzed for potential binding elements for FOX or SMAD family members. The potential FOX binding element (FBE) or SMAD binding element (SBE) identified with the Universal PBM Resource for Oligonucleotide Binding Evaluation (UniPROBE) database (63) within 1 kb upstream of CYP19 promoter from the translation start site is shown in Fig. 4. A sequence of 823 bp, which includes five FBEs (FBE1 to FBE5) and one SBE, was chosen for the construction of a luciferase reporter (-823/CYP19-Luc; inset in Fig. 5). The relative luciferase activity of -823/CYP19-Luc in HGrC1 cells following transfection with SMAD3, FOXL2^{wt}, and FOXL2^{C134W} plasmids (or matched empty vectors) is shown in Fig. 5. When expressed singly, neither FOXL2^{wt} nor FOXL2^{C134W} significantly activates -823/CYP19-Luc compared with the control. However, the simultaneous expression of FOXL2^{C134W} and SMAD3 significantly activated CYP19 promoter activity. These data suggest that the induction of CYP19 mRNA expression by FOXL2^{C134W} and SMAD3 observed in HGrC1 cells occurs at the transcriptional level.

FBE5 is required to stimulate CYP19 transcription by FOXL2^{C134W} and SMAD3

To analyze which sites were necessary for the enhanced transcriptional activity observed, we next constructed a series of truncated luciferase reporters from the -823/CYP19-Luc and evaluated their activities in HGrC1 cells expressing SMAD3, FOXL2^{wt}, and FOXL2^{C134W} alone or in combination (Fig. 6). The ratio of relative luciferase activity between FOXL2^{C134W} and FOXL2^{wt}

ACCTGGCTGAAAAGACAGATTCAATGGCATGTTGAAAAACACAGCAGAACCAGCACATCAGACTGTAAATTGATTGTCTTGCACAGGATGTTAGC
TGCTCTTCGAATGAGGTTCCTGAGTGGCACCTGAGCCTATTGCTGGTGGCATCCTATTCTGCCTGTTCTCTCT **FBE1** CTTCCCCATTCCT
TTCATTCTCTTCTCCCTTATTCTTCCTCTGCAATTCTTTTTTTCCACACTACCGTTGGCCGGTCCCTAGGGATACTGTTTAATCTGGCCCATGGT
ACAAGAGATTTTAGATCTTCATTGAAGTCACTAGAGATGGCCTGAGTGAGTCACTTTGAATTCAATAGACAAACTGATGGAAGGCTCTGAGAAGA
CCT **FBE2** CCAAGAAATGTGTTCTTACTGTAGAAACTTACT **FBE3** AAAAAAGTCATTTTGGTCAAAAAGGGGAGTTGGGAGATTGC
CTTTTTGTTTTGAAATTGATTTGGCTTCAAGGGAAGAAGATTGCCTAAACAAAACCTGCTGATGAAGTCACAAAATGACTCCACCTCTGGAATGA
GCTTTATTTTTCTTATAATTTGGCAAGAAATTTGGCTTTCAATTGGGAATGCACGTCACTCTACCCACTCAAGGGCAAGATGA **FBE5** ATCA
GA **FBE4** TAAAGGAACCTGA **SBE** CAAGGTCAGAAATGCTGCAATTCAAGCCAAAAGATCTTTCTTGGGCTTCCTTGTTTTGACTTG
TAACCATAAATTAGTCTTGCCTAAATGTCTGATCACATTATAAAACAGTAAGTGAATCTGTACTGTACAGCACCCTCTGAAGCAACAGGAGCTAT
AGATGAACCTTTTAGGGGATTCTGTAATTTTTCTGTCCCTTTGATTTCCACAGGACTCTAAATTGCCCCCTCTGAGGTCAAGGAACACAAGATGG
TTTTGGAAATGCTGAACCCGATACATTATAACATCACCAGCATCGTGCCTGAAGCCATGCCTGCTGCCACCATGCCAGTCCTGCTCCTCACTGGC

Figure 4. Potential binding sites of FOX (FBE) and SMAD (SBE) in the promoter region of human CYP19. Human CYP19 promoter region was analyzed by the Universal PBM Resource for Oligonucleotide Binding Evaluation (UniPROBE) database that hosts data generated by universal protein-binding microarray technology on the *in vitro* DNA binding specificities of proteins. The coding sequence is underlined.

is shown in the right panel of Fig. 6(a). Differential regulation of luciferase activity by FOXL2^{wt} and FOXL2^{C134W} was not observed in the absence of SMAD3 (white bars). By contrast, in the presence of SMAD3 (gray bars), all constructs except the most proximal (-56/CYP19-Luc) demonstrated significant differences between FOXL2^{wt} and FOXL2^{C134W}. These results suggested that either the FBE5 or SBE might distinguish the activities of FOXL2^{wt} vs FOXL2^{C134W} in regulating CYP19 transcription in the presence of SMAD3. We mutated six bases in either the SBE or FBE5 in the -823/CYP19-Luc construct and examined their activities [Fig. 6(b)]. Interestingly, the SBE mutant (left panel) maintained differential activity, whereas the FBE5 mutant (right panel) failed to exhibit selective induction by FOXL2^{C134W}, indicating that FBE5 is sufficient to distinguish between the activities by FOXL2^{wt} and FOXL2^{C134W}.

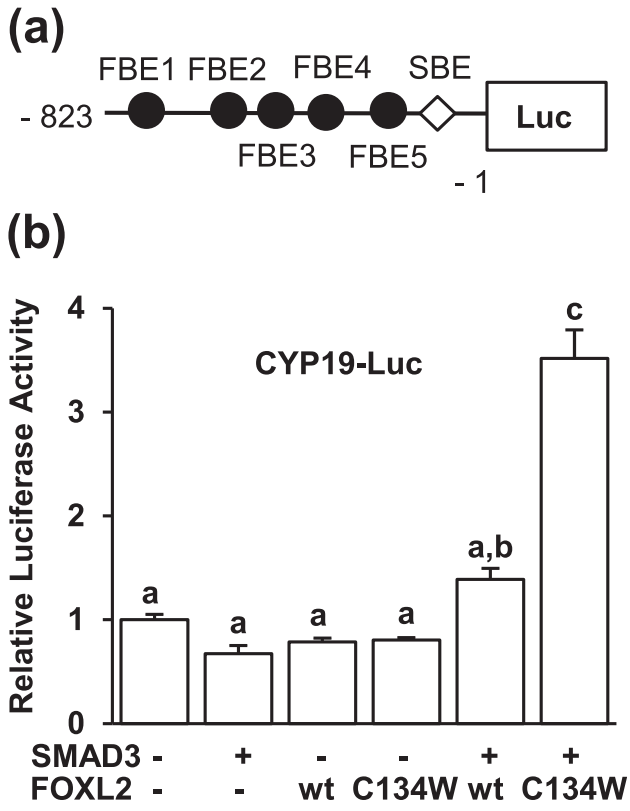

Figure 5. Human CYP19 promoter activity controlled by SMAD3 and FOXL2. (a) Luciferase construct of human CYP19 promoter. Potential FBE and SBE are shown. HGrC1 cells were transfected with the CYP19-luciferase reporter and indicated plasmid combinations of SMAD3 and Flag-FOXL2^{wt} or Flag-FOXL2^{C134W}. Empty expression vectors for SMAD3 and for Flag-FOXL2 were added as necessary to equalize the amount of plasmid transfected per well. After 4 hours, serum-free medium was replaced and cells were cultured for 24 hours. (b) qRT-PCR was performed to measure CYP19 mRNA levels. Representative results (n = 3) from triplicate experiments are presented. Data are shown as mean ± SEM. Different letters denote significant difference among experimental conditions ($P < 0.05$). Luc, luciferase; wt, wild-type.

FOXL2^{C134W} forms a more stable complex with SMAD3 than FOXL2^{wt} in HGrC1 cells

The reporter truncation analysis results implicated no role for the SBE, consistent with a lack of a role for SMAD2 in CYP19 expression. However, SMAD3 was critical for the difference in CYP19 expression by FOXL2^{C134W} inferring an alternative function of SMAD3. To investigate a possible interaction between FOXL2 and SMAD3, cells were again transfected with combinations of SMAD3, FOXL2^{wt}, and FOXL2^{C134W} plasmids, and immunoprecipitations were performed and analyzed by western blot. Figure 7 shows the levels of SMAD3 coprecipitated with FOXL2^{wt} or FOXL2^{C134W} (top panel) along with the input levels of SMAD3, FOXL2^{wt}, or FOXL2^{C134W} (middle and bottom panels). Despite equal or greater expression by FOXL2^{wt}, the interaction of SMAD3 was more intense with FOXL2^{C134W} than FOXL2^{wt} ($P < 0.05$), suggesting a more stable complex formed with FOXL2^{C134W} than FOXL2^{wt}.

FOXL2^{C134W} binds to FBE5 with a more stable interaction than FOXL2^{wt} in HGrC1 cells

To further investigate whether FOXL2^{C134W} directly binds to the FBE5 in the proximal promoter of CYP19, we performed oligonucleotide precipitation assays with probes that include intact or mutated FBE5 and SBE sites [Fig. 8(a)]. Cells expressing combinations of SMAD3, FOXL2^{wt}, and FOXL2^{C134W} plasmids were treated with activin A for 24 hours, lysed, and subjected to precipitation

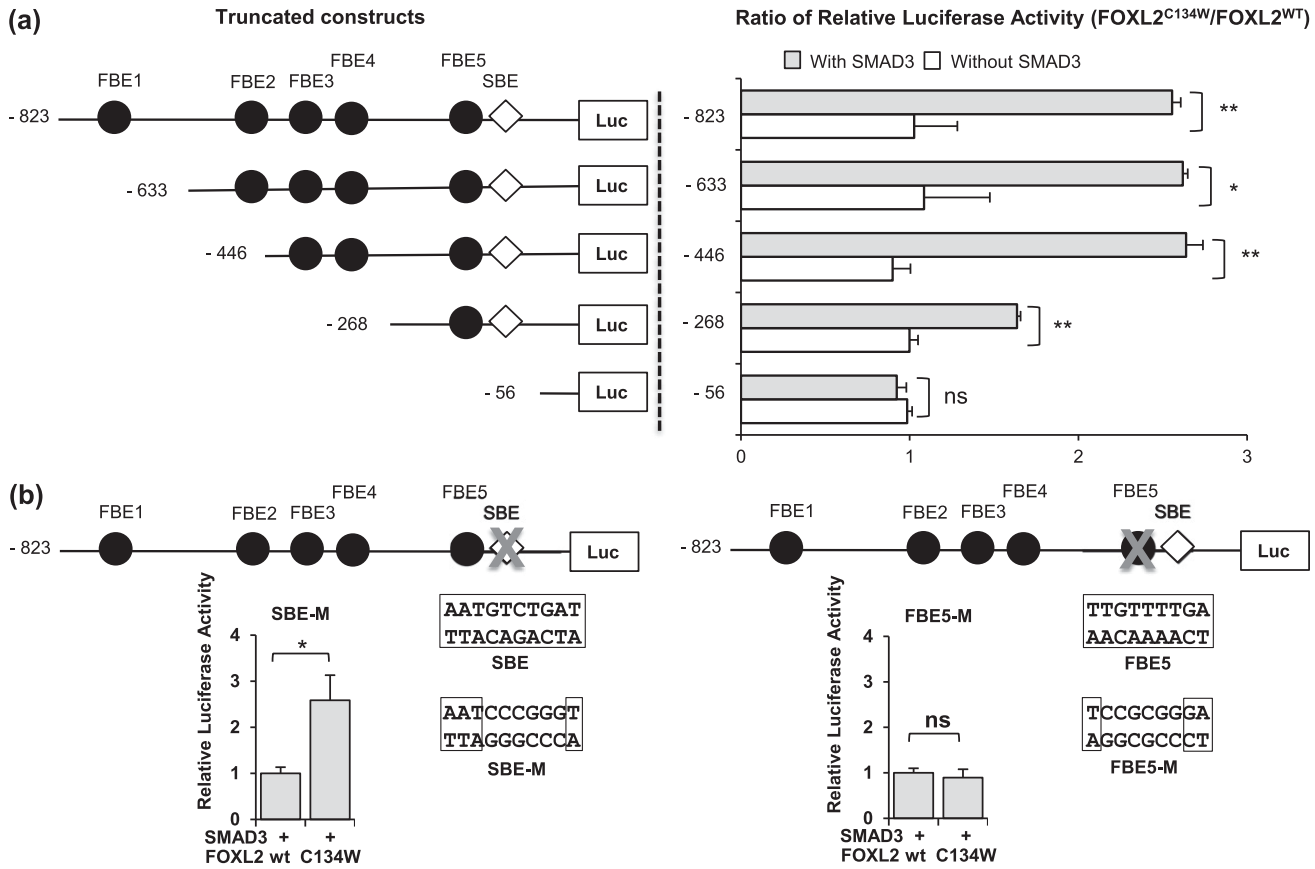

Figure 6. Luciferase activities of truncated constructs of human CYP19 promoter. (a) HGrC1 cells were transfected with an indicated CYP19-luciferase reporter and Flag-FOXL2^{wt} or Flag-FOXL2^{C134W} with (gray bars) or without (white bars) SMAD3 plasmid. Ratio of relative luciferase activities on the effect of FOXL2^{wt} or FOXL2^{C134W} are shown. (b) Contribution of the SBE or FBE5 to SMAD3 and FOXL2^{C134W} activation of CYP19 transcription. SBE and FBE5 sites were mutated in six internal bases (sequence not included in the box) within the -823/CYP19-luciferase reporter and tested for activation of luciferase transcription by FOXL2^{wt} or FOXL2^{C134W} and SMAD3. Relative luciferase activities are shown. Representative results (n = 3) from triplicate experiments are presented. Data are shown as mean ± SEM. The asterisks denote a significant difference among experimental conditions (*$P < 0.05$; **$P < 0.01$). Luc, luciferase; ns, not significant; wt, wild-type.

studies. FOXL2^{C134W} was more efficiently precipitated with FBE5/SBE than FOXL2^{wt} [Fig. 8(b), left panel; $P < 0.05$], although the input levels of FOXL2^{wt} and FOXL2^{C134W} were equal. However, when FBE5 was mutated (FBE5-M/SBE), the precipitated levels of both FOXL2^{wt} and FOXL2^{C134W} were dramatically reduced [Fig. 8(b), right panel]. Interestingly, the probe mutated at SBE (FBE5/SBE-M) did not alter FOXL2^{wt} or FOXL2^{C134W} binding to FBE5 relative to the FBE5/SBE probe ($P < 0.05$). These findings provide additional evidence that FBE5 is a binding site for FOXL2 and that C134W mutation confers more stability to FBE5 binding by FOXL2^{C134W} relative to FOXL2^{wt}, suggesting that FBE5 is essential for the differential activation of CYP19 transcription by FOXL2^{C134W} in HGrC1 cells.

Discussion

To study the molecular mechanisms underlying human GC function, GCs from *in vitro* fertilization patients have been widely used. However, there are substantial limitations in using *in vitro* fertilization GCs due to limited number of pooled GCs from several follicles that may have different gene expression profiles. Also, they are fully luteinized and do not survive in culture for an extended period. Reliable immortalized GCs are necessary as reproducible models of GC function. In the current study, experiments were carried out using a newly established, nonluteinized human GC cell line, HGrC1 (59). This cell line was established from GCs of the normal right ovary from a patient with monolateral mucinous adenocarcinoma at the left ovary and exhibits features of normal GCs at the early antral follicle stage expressing P450 aromatase and other GC-specific markers (59, 64). Thus, the HGrC1 cell line is distinct from other GCT-derived cell lines such as KGN and COV434 and may be more suitable to use in studies to extrapolate data obtained with the rodent to the human model. In fact, KGN cells are heterozygous for FOXL2^{C134W}, whereas COV434 cells have a defect in FOXL2 gene transcription (52). In contrast, our current study found that HGrC1 cells are homozygous for FOXL2^{wt}.

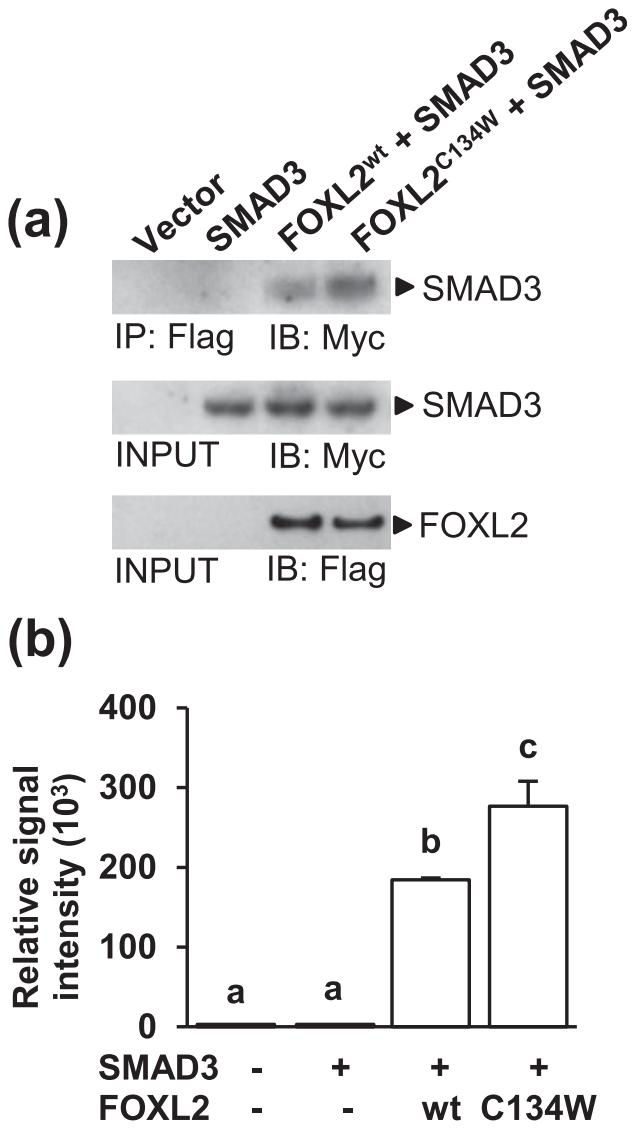

Figure 7. Protein-protein interactions between SMAD3 and FOXL2^{wt} or FOXL2^{C134W}. HGrC1 cells were transfected with combinations of Myc-SMAD3, Flag-FOXL2^{wt}, and Flag-FOXL2^{C134W} plasmids. Empty expression vectors for Myc-SMAD3 and for Flag-FOXL2 were added as necessary to equalize the amount of plasmid transfected per well. After 4 hours, serum-free medium was replaced and cells were cultured for 24 hours. (a) Protein lysates were immunoprecipitated with anti-Flag agarose beads, and SMAD3 proteins were detected with anti-Myc antibody. Levels of SMAD3 and FOXL2 proteins in the lysates before immunoprecipitation (INPUT) were detected with anti-Myc and anti-Flag antibodies, respectively. (b) Relative signal intensities of SMAD3 protein coprecipitated with FOXL2 were measured. Representative results from triplicate experiments are presented. Data are shown as mean ± SEM. Different letters denote significant difference among experimental conditions ($P < 0.05$). IB, immunoblotting; IP, immunoprecipitation; wt, wild-type.

Using HGrC1 cells, we present data that FOXL2^{wt} has no effect on CYP19 mRNA expression regardless of activin A treatment or SMAD3 overexpression. However, FOXL2 is known to repress many genes regulated by follicle-stimulating hormone, including CYP19, in CHO, KGN, and mouse primary GCs (65–67). FOXL2 downregulates CYP19 expression in CHO cells (65) but upregulates CYP19 expression in COS7 cells and ovine primary GCs (68) as well as in Japanese flounder (69) and tilapia (70). Therefore, FOXL2 regulation of CYP19 expression is controversial; the activity depends on the different cell types and species used in the study.

Our key finding is that FOXL2^{C134W}, but not FOXL2^{wt}, is able to induce CYP19 mRNA expression by an impressive 50-fold in the presence, but not absence, of activin A. Importantly, this was a functional change, as it corresponded to a 20-fold enhancement in estrogen level. This provides one mechanism to explain the increased levels of estrogen in women with aGCT. We further noted an eightfold increase in CYP19 when combined with SMAD3 expression. In fact, the eightfold increase would be remarkable if it were not overshadowed by the effect of FOXL2^{C134W} with activin A. This is a transcriptionally regulated process, because CYP19 promoter activity was also stimulated in a similar way. These data are in line with previously reported results by Fleming *et al.* (16), in which FOXL2^{C134W} was seen to increase CYP19 transcription compared with FOXL2^{wt}. This occurred via a single, highly conserved FOXL2 binding site, but in association with "unknown cofactor(s)." We show here that SMAD3 is a cofactor that differentially regulates CYP19 transcription in a manner dependent upon its partner, FOXL2^{C134W} or FOXL2^{wt}. This was not broadly true of all SMADs, as SMAD2 failed to regulate CYP19 transcription in HGrC1 cells. Moreover, we found that FOXL2^{C134W} binds FBE5 in CYP19 promoter more frequently or more firmly than FOXL2^{wt} and induces CYP19 promoter activity in the presence of SMAD3.

In the Co-IP assays (Fig. 7), FOXL2^{C134W} exhibited more stable interactions with SMAD3 compared with FOXL2^{wt}. However, we were unable to detect SMAD3 protein in the oligonucleotide coprecipitation assays despite our numerous attempts, including not only variations of experimental conditions, but also use of multiple inhibitors of alkaline phosphatase and a SMAD3 tagged with six copies of Myc to amplify our sensitivity relative to SMAD3 with one Myc epitope. The difference between biological and biochemical outcomes could be attributed to the difference in their experimental sensibilities. Thus, the precise mechanism by which SMAD3 is involved in the mechanism of FOXL2^{C134W}-induced CYP19 expression is not fully elucidated. However, our current data led us to propose a possible mechanism by which FOXL2^{C134W} and FOXL2^{wt} differently regulate CYP19 transcription with SMAD3 in HGrC1 cells as depicted in Fig. 9. Our data and proposed mechanism support the model described by Li *et al.* (71), in which

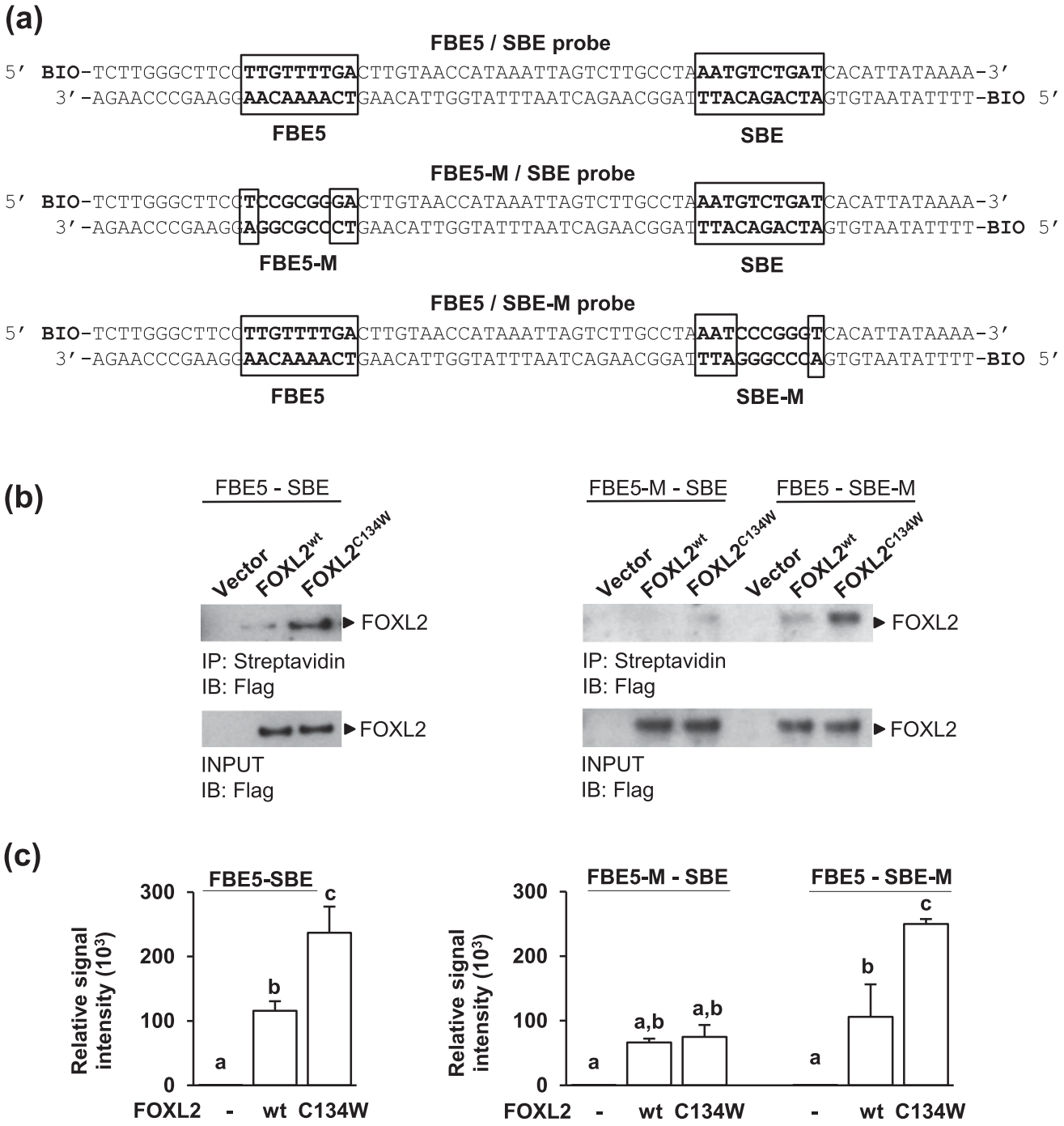

Figure 8. Oligonucleotide precipitation assay. (a) Biotinylated oligonucleotide probes were used for precipitation assays. FBE5 and SBE sites are boxed. FBE5-M and SBE-M are mutated FBE5 and SBE, respectively. (b) HGrC1 cells were transfected with Flag-FOXL2^{wt} or Flag-FOXL2^{C134W} plus Myc-SMAD3 plasmids. Empty expression vectors were added as necessary to equalize the amount of plasmid transfected per well. After 4 hours, serum-free medium was replaced, and cells were cultured in the presence or absence of 100 ng/mL activin A for 24 hours followed by the collection of cell lysates. Protein lysates were immunoprecipitated with each probe precoupled to streptavidin-conjugated agarose beads, and FOXL2 protein was detected with an anti-Flag antibody. (c) Relative signal intensities of FOXL2 protein coprecipitated with streptavidin-conjugated agarose beads were measured. Representative results from triplicate experiments are presented. Data are shown as mean ± SEM. Different letters denote significant difference among experimental conditions ($P < 0.05$). IB, immunoblotting; IP, immunoprecipitation; wt, wild-type.

SMAD3 binds, through the MH2 domain, to FOXL2 and not to the DNA.

The Cys^{134} residue is located within the C-terminal region of the forkhead domain, required for both DNA binding (24) and interaction with SMAD3 (37). Considering this, it is conceivable that the C134W mutation may cause more stable interactions of FOXL2 with both FBE5 and SMAD3, resulting in the excessive expression of CYP19. A potential role for a GC mitogen, activin A, in the pathogenesis of GCTs is also plausible as

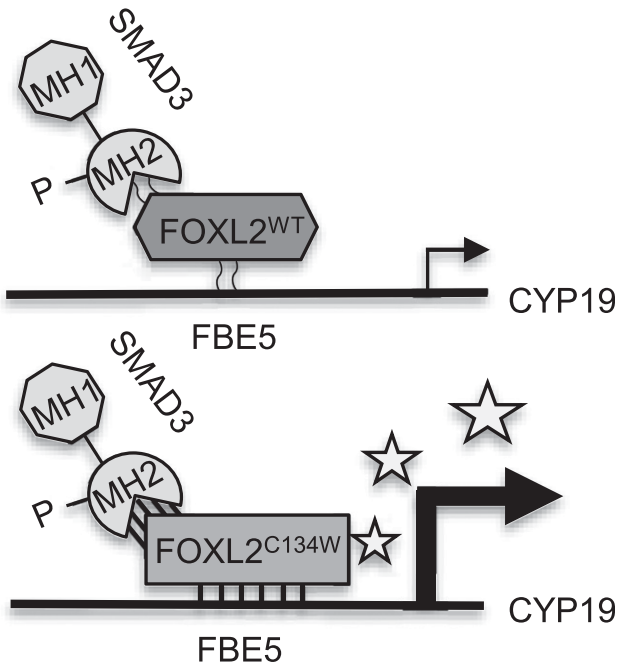

Figure 9. A possible mechanism for the regulation of *CYP19* transcription by FOXL2^{C134W} and SMAD3. Collective data in the current study support that FOXL2^{C134W} and SMAD3 synergistically stimulate *CYP19* transcription by binding to FBE5 in *CYP19* promoter more strongly than FOXL2^{wt} and SMAD3.

activation of SMAD3 has been implicated in the pathogenesis of GCTs (42).

CYP19 expression is a hallmark of aGCT, and serum E_2 levels are elevated in aGCT patients. There is not always a correlation between E_2 levels and the progression or recurrence of aGCTs (72, 73), which may relate to a lack of theca cells in the tumor stroma of certain aGCTs (74). In these patients, it is possible that, E_2 levels are normal yet CYP19 mRNA or protein levels are elevated. Additionally, serum inhibin B levels are markedly raised in women with aGCT (72, 75). However, neither FOXL2^{wt} nor FOXL2^{C134W} regulated INHBB mRNA when cells were treated with or without activin A, or in the presence or absence of SMAD3 overexpression [Fig. 1(b) and Fig. 2(b)]. Nevertheless, our findings in the HGrC1 cells do not exclude the possibility that FOXL2^{C134W} is linked to the elevated level of inhibin B *in vivo* in aGCT patients.

Blount *et al.* (37) uncovered a synergistic effect of FOXL2 and SMAD3 in enhancing activin A stimulation of follistatin expression in the pituitary. We later reported that downregulation of endogenous FOXL2 in rat primary GCs resulted in increased follistatin mRNA expression, suggesting that, in contrast to the report in pituitary cells, FOXL2 is inhibitory in follistatin expression in the ovary (41). Also, we showed that FOXL2 inhibits GDF9-induced follistatin transcription whereas FOXL2^{C134W} is more potent than FOXL2^{wt} in the inhibition in rat primary GCs. In the presence of SMAD3 overexpression, their inhibitory activities were more prominent (41). The synergistic suppression of follistatin transcription by FOXL2^{C134W} and SMAD3 was also demonstrated in our COV434 cell model (40). Further, in KGN cells, FOXL2^{wt}, but not FOXL2^{C134W}, stimulates follistatin mRNA expression (55). Thus, transcriptional activity of FOXL2 seems likely to be cell-type dependent, which may reflect a different subpopulation of transcriptional partners (41). Our finding that the *FOXL2* genes at both alleles in HGrC1 cells are intact and lack mutations would be useful information for the studies exploring the role of FOXL2^{C134W} in GC functions.

In summary, we have used HGrC1 cells to investigate the role of FOXL2^{C134W} mutation in GC function and found that (1) FOXL2^{C134W} stimulates CYP19 mRNA expression in the presence, but not absence, of activin A or SMAD3 overexpression, whereas FOXL2^{wt} does not regulate CYP19 mRNA expression regardless of the presence of activin A or SMAD3 in HGrC1 cells; (2) SMAD2 does not cooperate with FOXL2^{C134W} in stimulating CYP19 mRNA expression: (3) FOXL2^{C134W}, but not FOXL2^{wt}, stimulates CYP19 promoter in the presence of SMAD3 overexpression and FBE5 site is necessary for this transcriptional activation; and (4) FOXL2^{C134W} interacts with both SMAD3 and FBE5 more strongly than FOXL2^{wt}. This study demonstrates that SMAD3 is essential for FOXL2^{C134W} stimulation of CYP19 expression in HGrC1 cells, a synergistic action that is not observed in the presence of FOXL2^{wt} and SMAD2. The ability conferred by the C134W mutation to FOXL2 to bind DNA and partner proteins more stably might explain the altered CYP19 transcriptional activity and the excess of estrogen in aGCT patients.

Acknowledgments

We thank Dr. Louise Bilezikjian for the FOXL2^{wt} expression plasmid, Dr. Kohei Miyazono for providing us with the original SMAD2 and SMAD3 complementary DNA clones, and Dr. Lingzhi Zhang for technical assistance.

Financial Support: This work was supported by National Institutes of Health Grant P50HD012303 (to S.S.) and by University of California, San Diego Department of Reproductive Medicine Fund 60121B (to S.S.).

Correspondence: Shunichi Shimasaki, PhD, Department of Reproductive Medicine, School of Medicine, University of California, San Diego, 9500 Gilman Drive, La Jolla, California 92093. E-mail: sshimasaki@ucsd.edu.

Disclosure Summary: The authors have nothing to disclose.

References

1. Cocquet J, Pailhoux E, Jaubert F, Servel N, Xia X, Pannetier M, De Baere E, Messiaen L, Cotinot C, Fellous M, Veitia RA. Evolution and expression of FOXL2. *J Med Genet*. 2002;**39**(12):916–921.
2. Crisponi L, Deiana M, Loi A, Chiappe F, Uda M, Amati P, Bisceglia L, Zelante L, Nagaraja R, Porcu S, Ristaldi MS, Marzella R, Rocchi M, Nicolino M, Lienhardt-Roussie A, Nivelon A, Verloes A, Schlessinger D, Gasparini P, Bonneau D, Cao A, Pilia G. The putative forkhead transcription factor FOXL2 is mutated in blepharophimosis/ptosis/epicanthus inversus syndrome. *Nat Genet*. 2001;**27**(2):159–166.
3. Cocquet J, De Baere E, Gareil M, Pannetier M, Xia X, Fellous M, Veitia RA. Structure, evolution and expression of the FOXL2 transcription unit. *Cytogenet Genome Res*. 2003;**101**(3-4):206–211.
4. Ellsworth BS, Egashira N, Haller JL, Butts DL, Cocquet J, Clay CM, Osamura RY, Camper SA. FOXL2 in the pituitary: molecular, genetic, and developmental analysis. *Mol Endocrinol*. 2006;**20**(11): 2796–2805.
5. Loffler KA, Zarkower D, Koopman P. Etiology of ovarian failure in blepharophimosis ptosis epicanthus inversus syndrome: FOXL2 is a conserved, early-acting gene in vertebrate ovarian development. *Endocrinology*. 2003;**144**(7):3237–3243.
6. Pisarska MD, Bae J, Klein C, Hsueh AJ. Forkhead l2 is expressed in the ovary and represses the promoter activity of the steroidogenic acute regulatory gene. *Endocrinology*. 2004;**145**(7): 3424–3433.
7. Schmidt D, Ovitt CE, Anlag K, Fehsenfeld S, Gredsted L, Treier AC, Treier M. The murine winged-helix transcription factor Foxl2 is required for granulosa cell differentiation and ovary maintenance. *Development*. 2004;**131**(4):933–942.
8. Governini L, Carrarelli P, Rocha AL, Leo VD, Luddi A, Arcuri F, Piomboni P, Chapron C, Bilezikjian LM, Petraglia F. FOXL2 in human endometrium: hyperexpressed in endometriosis. *Reprod Sci*. 2014;**21**(10):1249–1255.
9. Uda M, Ottolenghi C, Crisponi L, Garcia JE, Deiana M, Kimber W, Forabosco A, Cao A, Schlessinger D, Pilia G. Foxl2 disruption causes mouse ovarian failure by pervasive blockage of follicle development. *Hum Mol Genet*. 2004;**13**(11):1171–1181.
10. Uhlenhaut NH, Jakob S, Anlag K, Eisenberger T, Sekido R, Kress J, Treier AC, Klugmann C, Klasen C, Holter NI, Riethmacher D, Schütz G, Cooney AJ, Lovell-Badge R, Treier M. Somatic sex reprogramming of adult ovaries to testes by FOXL2 ablation. *Cell*. 2009;**139**(6):1130–1142.
11. Leung DT, Fuller PJ, Chu S. Impact of FOXL2 mutations on signaling in ovarian granulosa cell tumors. *Int J Biochem Cell Biol*. 2016;**72**:51–54.
12. Dipietromaria A, Benayoun BA, Todeschini AL, Rivals I, Bazin C, Veitia RA. Towards a functional classification of pathogenic FOXL2 mutations using transactivation reporter systems. *Hum Mol Genet*. 2009;**18**(17):3324–3333.
13. De Baere E, Fellous M, Veitia RA. The transcription factor FOXL2 in ovarian function and dysfunction. *Folia Histochem Cytobiol*. 2009;**47**(5):S43–S49.
14. Shah SP, Köbel M, Senz J, Morin RD, Clarke BA, Wiegand KC, Leung G, Zayed A, Mehl E, Kalloger SE, Sun M, Giuliany R, Yorida E, Jones S, Varhol R, Swenerton KD, Miller D, Clement PB, Crane C, Madore J, Provencher D, Leung P, DeFazio A, Khattra J, Turashvili G, Zhao Y, Zeng T, Glover JN, Vanderhyden B, Zhao C, Parkinson CA, Jimenez-Linan M, Bowtell DD, Mes-Masson AM, Brenton JD, Aparicio SA, Boyd N, Hirst M, Gilks CB, Marra M, Huntsman DG. Mutation of FOXL2 in granulosa-cell tumors of the ovary. *N Engl J Med*. 2009;**360**(26):2719–2729.
15. Zannoni GF, Improta G, Petrillo M, Pettinato A, Scambia G, Fraggetta F. FOXL2 molecular status in adult granulosa cell tumors of the ovary: A study of primary and metastatic cases. *Oncol Lett*. 2016;**12**(2):1159–1163.
16. Fleming NI, Knower KC, Lazarus KA, Fuller PJ, Simpson ER, Clyne CD. Aromatase is a direct target of FOXL2: C134W in granulosa cell tumors via a single highly conserved binding site in the ovarian specific promoter. *PLoS One*. 2010;**5**(12):e14389.
17. Benayoun BA, Anttonen M, L'Hôte D, Bailly-Bechet M, Andersson N, Heikinheimo M, Veitia RA. Adult ovarian granulosa cell tumor transcriptomics: prevalence of FOXL2 target genes misregulation gives insights into the pathogenic mechanism of the p.Cys134Trp somatic mutation. *Oncogene*. 2013;**32**(22):2739–2746.
18. Anttonen M, Pihlajoki M, Andersson N, Georges A, L'hôte D, Vattulainen S, Färkkilä A, Unkila-Kallio L, Veitia RA, Heikinheimo M. FOXL2, GATA4, and SMAD3 co-operatively modulate gene expression, cell viability and apoptosis in ovarian granulosa cell tumor cells. *PLoS One*. 2014;**9**(1):e85545.
19. Kim JH, Kim YH, Kim HM, Park HO, Ha NC, Kim TH, Park M, Lee K, Bae J. FOXL2 posttranslational modifications mediated by GSK3β determine the growth of granulosa cell tumours. *Nat Commun*. 2014;**5**:2936.
20. Caburet S, Anttonen M, Todeschini AL, Unkila-Kallio L, Mestivier D, Butzow R, Veitia RA. Combined comparative genomic hybridization and transcriptomic analyses of ovarian granulosa cell tumors point to novel candidate driver genes. *BMC Cancer*. 2015; **15**(1):251.
21. Jamieson S, Fuller PJ. Molecular pathogenesis of granulosa cell tumors of the ovary. *Endocr Rev*. 2012;**33**(1):109–144.
22. Batista F, Vaiman D, Dausset J, Fellous M, Veitia RA. Potential targets of FOXL2, a transcription factor involved in craniofacial and follicular development, identified by transcriptomics. *Proc Natl Acad Sci USA*. 2007;**104**(9):3330–3335.
23. Benayoun BA, Batista F, Auer J, Dipietromaria A, L'Hôte D, De Baere E, Veitia RA. Positive and negative feedback regulates the transcription factor FOXL2 in response to cell stress: evidence for a regulatory imbalance induced by disease-causing mutations. *Hum Mol Genet*. 2009;**18**(4):632–644.
24. Benayoun BA, Caburet S, Dipietromaria A, Georges A, D'Haene B, Pandaranayaka PJ, L'Hôte D, Todeschini AL, Krishnaswamy S, Fellous M, De Baere E, Veitia RA. Functional exploration of the adult ovarian granulosa cell tumor-associated somatic FOXL2 mutation p.Cys134Trp (c.402C>G). *PLoS One*. 2010;**5**(1):e8789.
25. Benayoun BA, Kalfa N, Sultan C, Veitia RA. The forkhead factor FOXL2: A novel tumor suppressor? *Biochim Biophys Acta*. 2010; **1805**(1):1–5.
26. Benayoun BA, Georges AB, L'Hôte D, Andersson N, Dipietromaria A, Todeschini AL, Caburet S, Bazin C, Anttonen M, Veitia RA. Transcription factor FOXL2 protects granulosa cells from stress and delays cell cycle: role of its regulation by the SIRT1 deacetylase. *Hum Mol Genet*. 2011;**20**(9):1673–1686.
27. Caburet S, Georges A, L'Hôte D, Todeschini AL, Benayoun BA, Veitia RA. The transcription factor FOXL2: at the crossroads of ovarian physiology and pathology. *Mol Cell Endocrinol*. 2012; **356**(1-2):55–64.
28. Parker KL. Tissue-specific knockouts of steroidogenic factor 1. *Endocr Res*. 2004;**30**(4):855.
29. Park M, Shin E, Won M, Kim JH, Go H, Kim HL, Ko JJ, Lee K, Bae J. FOXL2 interacts with steroidogenic factor-1 (SF-1) and represses SF-1-induced CYP17 transcription in granulosa cells. *Mol Endocrinol*. 2010;**24**(5):1024–1036.
30. Ou Q, Mouillet JF, Yan X, Dorn C, Crawford PA, Sadovsky Y. The DEAD box protein DP103 is a regulator of steroidogenic factor-1. *Mol Endocrinol*. 2001;**15**(1):69–79.
31. Lee K, Pisarska MD, Ko JJ, Kang Y, Yoon S, Ryou SM, Cha KY, Bae J. Transcriptional factor FOXL2 interacts with DP103 and induces apoptosis. *Biochem Biophys Res Commun*. 2005;**336**(3): 876–881.
32. Lee MB, Lebedeva LA, Suzawa M, Wadekar SA, Desclozeaux M, Ingraham HA. The DEAD-box protein DP103 (Ddx20 or Gemin-3) represses orphan nuclear receptor activity via SUMO modification. *Mol Cell Biol*. 2005;**25**(5):1879–1890.

33. Kim MS, Hur SY, Yoo NJ, Lee SH. Mutational analysis of FOXL2 codon 134 in granulosa cell tumour of ovary and other human cancers. *J Pathol*. 2010;**221**(2):147–152.
34. Kim T, Sung CO, Song SY, Bae DS, Choi YL. FOXL2 mutation in granulosa-cell tumours of the ovary. *Histopathology*. 2010;**56**(3): 408–410.
35. Kim SY, Weiss J, Tong M, Laronda MM, Lee EJ, Jameson JL. Foxl2, a forkhead transcription factor, modulates nonclassical activity of the estrogen receptor-alpha. *Endocrinology*. 2009; **150**(11):5085–5093.
36. Ellsworth BS, Burns AT, Escudero KW, Duval DL, Nelson SE, Clay CM. The gonadotropin releasing hormone (GnRH) receptor activating sequence (GRAS) is a composite regulatory element that interacts with multiple classes of transcription factors including Smads, AP-1 and a forkhead DNA binding protein. *Mol Cell Endocrinol*. 2003;**206**(1-2):93–111.
37. Blount AL, Schmidt K, Justice NJ, Vale WW, Fischer WH, Bilezikjian LM. FoxL2 and Smad3 coordinately regulate follistatin gene transcription. *J Biol Chem*. 2009;**284**(12):7631–7645.
38. Lamba P, Fortin J, Tran S, Wang Y, Bernard DJ. A novel role for the forkhead transcription factor FOXL2 in activin A-regulated follicle-stimulating hormone beta subunit transcription. *Mol Endocrinol*. 2009;**23**(7):1001–1013.
39. Corpuz PS, Lindaman LL, Mellon PL, Coss D. FoxL2 is required for activin induction of the mouse and human follicle-stimulating hormone beta-subunit genes. *Mol Endocrinol*. 2010;**24**(5):1037–1051.
40. Nonis D, McTavish KJ, Shimasaki S. Essential but differential role of FOXL2wt and FOXL2C134W in GDF-9 stimulation of follistatin transcription in co-operation with Smad3 in the human granulosa cell line COV434. *Mol Cell Endocrinol*. 2013;**372**(1-2): 42–48.
41. McTavish KJ, Nonis D, Hoang YD, Shimasaki S. Granulosa cell tumor mutant FOXL2C134W suppresses GDF-9 and activin A-induced follistatin transcription in primary granulosa cells. *Mol Cell Endocrinol*. 2013;**372**(1-2):57–64.
42. Fang X, Gao Y, Li Q. SMAD3 activation: a converging point of dysregulated TGF-beta superfamily signaling and genetic aberrations in granulosa cell tumor development? *Biol Reprod*. 2016; **95**(5):105.
43. Alexiadis M, Chu S, Leung D, Gould JA, Jobling T, Fuller PJ. Transcriptomic analysis of stage 1 versus advanced adult granulosa cell tumors. *Oncotarget*. 2016;**7**(12):14207–14219.
44. Suh DS, Oh HK, Kim JH, Park S, Shin E, Lee K, Kim YH, Bae J. Identification and validation of differential phosphorylation sites of the nuclear FOXL2 protein as potential novel biomarkers for adult-type granulosa cell tumors. *J Proteome Res*. 2015;**14**(6): 2446–2456.
45. Irusta G, Pazos MC, Abramovich D, De Zúñiga I, Parborell F, Tesone M. Effects of an inhibitor of the γ-secretase complex on proliferation and apoptotic parameters in a FOXL2-mutated granulosa tumor cell line (KGN). *Biol Reprod*. 2013;**89**(1):9.
46. Jamieson S, Fuller PJ. Characterization of the inhibitor of kappaB kinase (IKK) complex in granulosa cell tumors of the ovary and granulosa cell tumor-derived cell lines. *Horm Cancer*. 2013;**4**(5): 277–292.
47. Cheng JC, Klausen C, Leung PC. Overexpression of wild-type but not C134W mutant FOXL2 enhances GnRH-induced cell apoptosis by increasing GnRH receptor expression in human granulosa cell tumors. *PLoS One*. 2013;**8**(1):e55099.
48. Rosario R, Blenkiron C, Shelling AN. Comparative study of microRNA regulation on FOXL2 between adult-type and juvenile-type granulosa cell tumours in vitro. *Gynecol Oncol*. 2013;**129**(1): 209–215.
49. Alexiadis M, Eriksson N, Jamieson S, Davis M, Drummond AE, Chu S, Clyne CD, Muscat GE, Fuller PJ. Nuclear receptor profiling of ovarian granulosa cell tumors. *Horm Cancer*. 2011;**2**(3):157–169.
50. Beysen D, Moumné L, Veitia R, Peters H, Leroy BP, De Paepe A, De Baere E. Missense mutations in the forkhead domain of FOXL2 lead to subcellular mislocalization, protein aggregation and impaired transactivation. *Hum Mol Genet*. 2008;**17**(13):2030–2038.
51. Schrader KA, Gorbatcheva B, Senz J, Heravi-Moussavi A, Melnyk N, Salamanca C, Maines-Bandiera S, Cooke SL, Leung P, Brenton JD, Gilks CB, Monahan J, Huntsman DG. The specificity of the FOXL2 c.402C>G somatic mutation: a survey of solid tumors. *PLoS One*. 2009;**4**(11):e7988.
52. Jamieson S, Butzow R, Andersson N, Alexiadis M, Unkila-Kallio L, Heikinheimo M, Fuller PJ, Anttonen M. The FOXL2 C134W mutation is characteristic of adult granulosa cell tumors of the ovary. *Mod Pathol*. 2010;**23**(11):1477–1485.
53. Rosario R, Araki H, Print CG, Shelling AN. The transcriptional targets of mutant FOXL2 in granulosa cell tumours. *PLoS One*. 2012;**7**(9):e46270.
54. Kim JH, Yoon S, Park M, Park HO, Ko JJ, Lee K, Bae J. Differential apoptotic activities of wild-type FOXL2 and the adult-type granulosa cell tumor-associated mutant FOXL2 (C134W). *Oncogene*. 2011;**30**(14):1653–1663.
55. Cheng JC, Chang HM, Qiu X, Fang L, Leung PC. FOXL2-induced follistatin attenuates activin A-stimulated cell proliferation in human granulosa cell tumors. *Biochem Biophys Res Commun*. 2014; **443**(2):537–542.
56. Wang T, Li F, Tang S. MiR-30a upregulates BCL2A1, IER3 and cyclin D2 expression by targeting FOXL2. *Oncol Lett*. 2015;**9**(2): 967–971.
57. Nishi Y, Yanase T, Mu Y, Oba K, Ichino I, Saito M, Nomura M, Mukasa C, Okabe T, Goto K, Takayanagi R, Kashimura Y, Haji M, Nawata H. Establishment and characterization of a steroidogenic human granulosa-like tumor cell line, KGN, that expresses functional follicle-stimulating hormone receptor. *Endocrinology*. 2001;**142**(1):437–445.
58. van den Berg-Bakker CAM, Hagemeijer A, Franken-Postma EM, Smit VTHBM, Kuppen PJK, van Ravenswaay Claasen HH, Cornelisse CJ, Schrier PI. Establishment and characterization of 7 ovarian carcinoma cell lines and one granulosa tumor cell line: growth features and cytogenetics. *Int J Cancer*. 1993;**53**(4):613–620.
59. Bayasula IA, Iwase A, Kiyono T, Takikawa S, Goto M, Nakamura T, Nagatomo Y, Nakahara T, Kotani T, Kobayashi H, Kondo M, Manabe S, Kikkawa F. Establishment of a human nonluteinized granulosa cell line that transitions from the gonadotropin-independent to the gonadotropin-dependent status. *Endocrinology*. 2012;**153**(6):2851–2860.
60. Otsuka F, Shimasaki S. A negative feedback system between oocyte bone morphogenetic protein 15 and granulosa cell kit ligand: its role in regulating granulosa cell mitosis. *Proc Natl Acad Sci USA*. 2002;**99**(12):8060–8065.
61. Kawabata M, Inoue H, Hanyu A, Imamura T, Miyazono K. Smad proteins exist as monomers in vivo and undergo homo- and hetero-oligomerization upon activation by serine/threonine kinase receptors. *EMBO J*. 1998;**17**(14):4056–4065.
62. Komuro A, Imamura T, Saitoh M, Yoshida Y, Yamori T, Miyazono K, Miyazawa K. Negative regulation of transforming growth factor-beta (TGF-beta) signaling by WW domain-containing protein 1 (WWP1). *Oncogene*. 2004;**23**(41):6914–6923.
63. Hume MA, Barrera LA, Gisselbrecht SS, Bulyk ML. UniPROBE, update 2015: new tools and content for the online database of protein-binding microarray data on protein-DNA interactions. *Nucleic Acids Res*. 2015;**43**(D1):D117–D122.
64. Nakamura T, Iwase A, Bayasula B, Nagatomo Y, Kondo M, Nakahara T, Takikawa S, Goto M, Kotani T, Kiyono T, Kikkawa F. CYP51A1 induced by growth differentiation factor 9 and follicle-stimulating hormone in granulosa cells is a possible predictor for unfertilization. *Reprod Sci*. 2015;**22**(3):377–384.
65. Bentsi-Barnes IK, Kuo FT, Barlow GM, Pisarska MD. Human forkhead L2 represses key genes in granulosa cell differentiation including aromatase, P450scc, and cyclin D2. *Fertil Steril*. 2010; **94**(1):353–356.

66. Kuo FT, Bentsi-Barnes IK, Barlow GM, Pisarska MD. Mutant Forkhead L2 (FOXL2) proteins associated with premature ovarian failure (POF) dimerize with wild-type FOXL2, leading to altered regulation of genes associated with granulosa cell differentiation. *Endocrinology*. 2011;**152**(10):3917–3929.
67. Kuo FT, Fan K, Bentsi-Barnes I, Barlow GM, Pisarska MD. Mouse forkhead L2 maintains repression of FSH-dependent genes in the granulosa cell. *Reproduction*. 2012;**144**(4):485–494.
68. Pannetier M, Fabre S, Batista F, Kocer A, Renault L, Jolivet G, Mandon-Pépin B, Cotinot C, Veitia R, Pailhoux E. FOXL2 activates P450 aromatase gene transcription: towards a better characterization of the early steps of mammalian ovarian development. *J Mol Endocrinol*. 2006;**36**(3):399–413.
69. Yamaguchi T, Yamaguchi S, Hirai T, Kitano T. Follicle-stimulating hormone signaling and Foxl2 are involved in transcriptional regulation of aromatase gene during gonadal sex differentiation in Japanese flounder, Paralichthys olivaceus. *Biochem Biophys Res Commun*. 2007;**359**(4):935–940.
70. Wang DS, Kobayashi T, Zhou LY, Paul-Prasanth B, Ijiri S, Sakai F, Okubo K, Morohashi K, Nagahama Y. Foxl2 up-regulates aromatase gene transcription in a female-specific manner by binding to the promoter as well as interacting with ad4 binding protein/steroidogenic factor 1. *Mol Endocrinol*. 2007;**21**(3):712–725.
71. Li Y, Schang G, Boehm U, Deng CX, Graff J, Bernard DJ. SMAD3 regulates follicle-stimulating hormone synthesis by pituitary gonadotrope cells in vivo. *J Biol Chem*. 2017;**292**(6):2301–2314.
72. Lappöhn RE, Burger HG, Bouma J, Bangah M, Krans M, de Bruijn HW. Inhibin as a marker for granulosa-cell tumors. *N Engl J Med*. 1989;**321**(12):790–793.
73. Rey RA, Lhommé C, Marcillac I, Lahlou N, Duvillard P, Josso N, Bidart JM. Antimüllerian hormone as a serum marker of granulosa cell tumorsof the ovary: comparative study with serum alpha-inhibin and estradiol. *Am J Obstet Gynecol*. 1996;**174**(3):958–965.
74. Schumer ST, Cannistra SA. Granulosa cell tumor of the ovary. *J Clin Oncol*. 2003;**21**(6):1180–1189.
75. Boggess JF, Soules MR, Goff BA, Greer BE, Cain JM, Tamimi HK. Serum inhibin and disease status in women with ovarian granulosa cell tumors. *Gynecol Oncol*. 1997;**64**(1):64–69.